NADPH as a co-substrate for studies of the chlorinating activity of myeloperoxidase

Françoise AUCHÈRE and Chantal CAPEILLÈRE-BLANDIN[1]

Laboratoire de chimie et biochimie pharmacologiques et toxicologiques, CNRS UMR 8601, Université René Descartes, Paris V, 45 rue des Saints Pères, 75270 Paris Cedex 06, France

The reinvestigation of the kinetics of myeloperoxidase (MPO) activity with the use of NADPH as a probe has allowed us to determine the effects of H_2O_2, Cl^- ion and pH on the MPO-dependent production of HOCl. The chlorination rate of NADPH did not depend on NADPH concentration and was entirely related to the rate of production of HOCl by MPO. The overall oxidation of NADPH occurred similarly in the absence of O_2 and was insensitive to scavengers of the superoxide radical anion. Experiments performed on the direct oxidation of NADPH by MPO in the presence and the absence of H_2O_2 showed that neither the rate nor the stoichiometry of the reaction could interfere in the NADPH oxidation process involved in the steady-state chlorination cycle. The oxidation of NADPH was characterized by a decrease in the A_{339} of the reduced nicotinamide with the concomitant appearance of a new chromophore with absorbance maximum at 274 nm, characterized by isosbestic points at 300 and 238 nm. The reaction product did not possess any enzymic properties with dehydrogenases and led to a metabolite other than $NADP^+$. Its amount accounted for a stoichiometric conversion of H_2O_2 into HOCl. Analyses of the NADPH reaction allowed the determination of both kinetic (k_{cat} and K_m) and thermodynamic (K_d) parameters. When the values of kinetic parameters were compared with previously published ones, the main discrepancy was found with data obtained with the chlorination of monochlorodimedon and a better agreement with diethanolchloramine formation or H_2O_2 consumption. Variations in the extent of NADPH oxidation with Cl^- concentration enabled us to determine the dissociation constant for the enzyme–Cl^- complex. In the course of titration studies, the spectral properties of NADPH reacting with either HOCl or the MPO/H_2O_2/Cl^- system were quantitatively similar in terms of stoichiometry and absorbance coefficient and thus led to identical chlorinated products. However, no spectral modification occurred with $NADP^+$ and adenine nucleotide analogues under the same conditions. A quantitative comparison of difference spectra obtained with NADPH and NMNH indicated that chlorination occurred on the nicotinamide part of the molecule.

Key words: chlorination, hypochlorous acid, NADPH co-oxidation.

INTRODUCTION

Hypochlorous acid (HOCl) generated by activated neutrophils and monocytes is considered to have a major role as a potent microbicidal agent in the immune defence [1]. This short-lived and diffusible oxidant can participate in a variety of secondary non-enzymic reactions, such as the oxidation and/or chlorination of target-cell components, in particular leading to inflammatory tissue damage [1,2]. Indeed, HOCl reacts with a wide range of oxidizable biomolecules containing thiols, nitrogen-containing compounds or unsaturated double carbon bonds [3]. They correspond to the main targets of HOCl oxidation in proteins [4,5], nucleotides [6–8] and unsaturated lipids and cholesterol [9,10].

Activated phagocytes contain the haem-enzyme myeloperoxidase (MPO), which catalyses the reaction of Cl^- ion with H_2O_2 to generate large amounts of HOCl during the respiratory burst [11]. In the chlorination cycle, native MPO reacts with H_2O_2 to form the active redox intermediate, compound I (C I). Then the high reduction potential of this intermediate enables MPO to oxidize Cl^- ion to free HOCl with the concomitant regeneration of native enzyme, as follows [12]:

$$MPO + H_2O_2 \rightarrow C\ I + H_2O \quad (1)$$

$$C\ I + H^+ + Cl^- \rightarrow MPO + HOCl \quad (2)$$

$$C\ I + AH_2 \rightarrow C\ II + AH^{\bullet} \quad (3)$$

$$C\ II + AH_2 \rightarrow MPO + AH^{\bullet} \quad (4)$$

$$MPO + O_2^{-\bullet} \rightarrow C\ III \quad (5)$$

where C II and C III are compound II and compound III respectively and $O_2^{-\bullet}$ is the superoxide radical anion.

Alternatively, in the presence of a reducing substrate, AH_2, or excess H_2O_2, C I could be converted into the redox intermediate C II via a one-electron step that concomitantly generates a free-radical product, $AH^{\bullet}$ or $O_2^{-\bullet}$ respectively [eqn. (3)]. The classical cycle is complete when C II is reduced back to native MPO by the reducing substrate [eqn. (4)] [12]. Moreover, the reaction of native MPO with $O_2^{-\bullet}$ leads to the oxyferrous form of the enzyme, namely C III [eqn. (5)]. Both C II and C III are inactive in the formation of HOCl.

The MPO-produced HOCl was found to easily oxidize L-ascorbic acid [13,14], 5-thio-2-nitrobenzoic acid (Nbs) [15], methionine [16], GSH [8,17] and more generally alkyl aryl sulphides [18], and to chlorinate diethanolamine [19], taurine [20,21] and monochlorodimedon (MCD) [22].

Because the formation of HOCl by MPO can only be measured indirectly, the chlorinating activity of MPO was monitored by spectrophotometric methods based on non-enzymic reactions mediated by HOCl with the use of a compound that changes absorbance on oxidation or chlorination. Most of the investigations on the chlorinating activity of MPO have been performed with the use of MCD [22–25]. Recently, L-ascorbic acid and Nbs were recommended for the direct monitoring of the oxidative effect of the MPO/H_2O_2/Cl^- system [14,15] but they were

Abbreviations used: C I, C II and C III, compound I, compound II and compound III; MCD, monochlorodimedon; MPO, myeloperoxidase; Nbs^{2-}, 5-thio-2-nitrobenzoic acid; NBT, Nitro Blue Tetrazolium; $O_2^{-\bullet}$, superoxide radical anion; SOD, superoxide dismutase; TNM, tetranitromethane.

[1] To whom correspondence should be addressed (e-mail blandin@biomedicale.univ-paris5.fr).

susceptible to interference. Indeed, L-ascorbic acid and MCD react with the enzyme intermediates in the absence of Cl^- and therefore influence the MPO activity [24–27]. With regard to interference with the Nbs assay, many reducing compounds, especially those containing free thiol groups, react with Nbs_2 (Ellman's reagent) and convert it back into Nbs.

The peroxidase-catalysed oxidation of halides into products that are known to react non-enzymically with NADPH has been described for MPO [7,28], chloroperoxidase [29] and lactoperoxidase [30]. The aim of the present study was to assess the use of NADPH to estimate the chlorinating activity of human MPO. Control experiments failed to show any contribution of the MPO oxidase reaction to the NADPH chloration reaction. Evidence for the occurrence of a reaction different from the oxidation to $NADP^+$ in the presence of free HOCl and HOCl generated by the $MPO/H_2O_2/Cl^-$ system was obtained by analyses of the coenzyme activities of the reaction products and by comparison of the spectral changes in the UV. The kinetics of the reaction of NADPH with the $MPO/H_2O_2/Cl^-$ system were investigated in further detail, and the influence of various parameters, pH, H_2O_2 and Cl^- concentrations, on the rate of NADPH disappearance was examined. The results tend to support the use of NADPH as a scavenger of HOCl generated by the $MPO/H_2O_2/Cl^-$ system.

MATERIALS AND METHODS

Chemicals

Glucose-6-phosphate dehydrogenase from baker's yeast, glucose oxidase type VII-S from *Aspergillus niger* and superoxide dismutase (SOD) from bovine erythrocytes were purchased from Sigma Chemical Co. (St. Louis, MO, U.S.A.). Tetranitromethane (TNM), Nitro Blue Tetrazolium (NBT), NADPH tetrasodium salt, NADH, NMNH, $NADP^+$, NAD^+, NMN, adenosine 2′,5′-diphosphate, ADP, MCD and guaiacol were obtained from Sigma. All other chemicals used were of the highest grade available and were prepared daily in distilled deionized water. All experiments were performed at 20 °C and, unless stated otherwise, the buffer used was 20 mM sodium/potassium phosphate buffer, pH 6.0.

MPO characteristics

MPO was purified from human polymorphonuclear neutrophils by the method described previously [31]. The enzyme preparation used in this study exhibited a purity index (A_{428}/A_{279}) equal to or greater than 0.81. The MPO concentration, expressed as haem concentration, was determined spectrophotometrically on the basis of the Soret absorbance at 428 nm by using a millimolar absorption coefficient per haem of 89 $mM^{-1}\cdot cm^{-1}$ [32]. The spectrophotometric characteristics of C I, C II and C III generated were in agreement with published spectra [33]. C III and C II were distinguished by the ratios of their absorbances at 626 and 454 nm (0.52 and 0.20 respectively) [33]. In routine assay, the standard molar activity (mean ± S.D.) of MPO was 400 ± 30 s^{-1} at 20 °C under typical reaction conditions consisting of a saturating concentration of 300 μM H_2O_2, 13.4 mM guaiacol and 20 nM MPO, in 20 mM phosphate buffer, pH 7.0.

Measurements of substrate and product concentrations

H_2O_2 stock solutions were prepared by appropriate dilutions of 30 % (v/v) H_2O_2 (Sigma) in triply distilled deionized water of conductivity 1.3 μS. Their concentrations were determined by absorbance measurements at 240 nm, taking ϵ_{240} as 43.6 $M^{-1}\cdot cm^{-1}$ [34]; the dilutions required were made daily.

Fresh solutions of $HOCl/OCl^-$ ($pK_a = 7.6$) were prepared by dilution of the commercial NaOCl before use. The OCl^- concentration was determined spectrophotometrically by measurement of A_{292} (ϵ_{292} 350 $M^{-1}\cdot cm^{-1}$) after dilution with 0.1 M NaOH [35].

To avoid the autoxidation of NADPH, stock solutions at 12 mM were made daily in triply distilled slightly alkaline water, defined by a conductivity measurement of 1.3 μS. Measurements with different solutions of commercially available NADPH revealed significant differences in terms of stability and presence of degradation products. The results reported here were obtained with solutions of Sigma β-NADPH tetrasodium salt characterized by a single peak after HPLC chromatography on an analytical Hypersil ODS column.

Spectral measurements

Absorbance spectra, repetitive scans and kinetic absorbance measurements were performed with a Perkin–Elmer λ 40 interfaced with a computer allowing the collection, manipulation and analysis of the data with the corresponding appropriate software. To monitor the possible generation of $O_2^{-\bullet}$, the reduction of NBT (25 μM) and ferricytochrome *c* (20 μM) was followed continuously at 560 nm (ϵ 15 $mM^{-1}\cdot cm^{-1}$) and 550 nm (ϵ 21 $mM^{-1}\cdot cm^{-1}$) respectively.

Reaction of NADPH with MPO in the presence or absence of H_2O_2

To control the stability of buffered NADPH solutions in the pH range 8–4 and the reactivity of C I and C II with 100 μM NADPH, time-dependent spectra were scanned at 960 nm/min during the reaction with 1 μM MPO in the absence or presence of 100 μM H_2O_2. The steady-state spectra during NADPH oxidation and chlorination were evaluated in the presence of a glucose–glucose oxidase system and recorded at 240 nm/min. Reaction was started by the addition of glucose oxidase to MPO and 45 mM glucose in air-saturated phosphate buffer (20 mM, pH 6.0). A constant flux of 5 μM H_2O_2/min was obtained at 90 ng/ml, corresponding to 13 m-units/ml. When necessary, anaerobic conditions were obtained by pre-gassing the solutions with argon.

Reaction of NADPH with MPO, H_2O_2 and Cl^-

Initial rates of NAD(P)H oxidation were determined with various concentrations of H_2O_2, Cl^- or NADPH, with 15–20 nM MPO in 20 mM phosphate buffer, pH 6.0 at 20 °C. The reaction was initiated by the addition of MPO; the rate of disappearance of NAD(P)H was monitored at 339 nm by using a millimolar absorption coefficient of 6.2 $mM^{-1}\cdot cm^{-1}$. For each concentration, measurements were made in duplicate. All experiments were repeated at least three times with different MPO preparations. The steady-state kinetic constants k_{cat} and K_m were determined by a direct fit of the non-inhibited part of the plot to the Michaelis–Menten equation with the use of a non-linear regression analysis program (Kaleidagraph 3.0). The following buffers were used at a concentration of 20 mM to test pH effects: acetate, pH 4–5; phosphate, pH 6–8.

Spectrophotometric titrations

The redox titrations of reduced nicotinamide nucleotides by HOCl, generated by the $MPO/H_2O_2/Cl^-$ system and/or free HOCl obtained by the addition of NaOCl, were monitored by repetitive scans performed between 450 and 200 nm at a rate of 240 nm/min, either in the presence of 100 mM NaCl and MPO

with the incremental addition of H_2O_2 (as specified in the Figure legends) or after the repetitive addition of HOCl aliquots. In the latter case, the absorbance changes were found to be essentially instantaneous, whereas in the former, three or four scans were recorded, i.e. taking 5 min, to obtain a stable absorbance before the next addition.

RESULTS

Steady-state kinetics of NADPH oxidation

Time-courses of NADPH oxidation by the MPO/H_2O_2/Cl^- system

Figure 1 illustrates the NADPH oxidation time courses catalysed by the MPO/H_2O_2/Cl^- system. In the presence of 100 mM NaCl (curve a), A_{339} decreased rapidly at a rate of 95 μM/min. The results of separate experiments performed under anaerobic and aerobic conditions indicated that the presence or absence of O_2 (curve b) did not influence the NADPH oxidation rate. Moreover, the addition of 10 μM TNM or 25 μM NBT, well-known scavengers of $O_2^{-\bullet}$, did not modify the time course of NADPH oxidation (curve c). For these time courses, the mean turnover rate was 85 ± 4 μM NADPH oxidized/s per μM haem enzyme. The complete disappearance of absorbance was obtained only for H_2O_2 concentrations equal to or greater than NADPH concentration. The addition of 5 mM glucose 6-phosphate and 0.1 μM glucose-6-phosphate dehydrogenase after complete NADPH oxidation did not allow the regeneration of NADPH, thus indicating that the oxidized species was not $NADP^+$, the active cofactor of the dehydrogenase.

NADPH stability in buffered solutions

To document the participation of NAD(P)H as an MPO oxidase substrate in the MPO-chlorinating activity, control experiments were performed. First, the stability of NADPH in buffered solutions between pH 8.0 and 4.0 was checked by monitoring

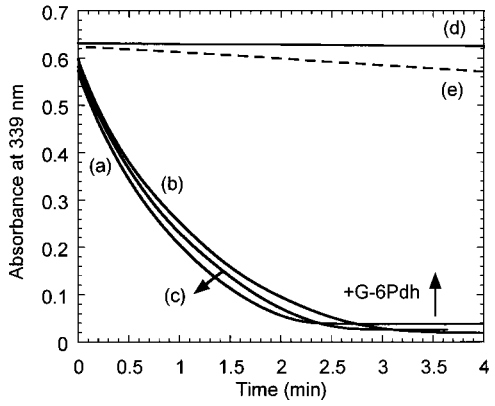

Figure 1 Time course of NADPH oxidation

The kinetics of disappearance of NADPH were followed at 339 nm. The reaction was initiated by the addition of MPO. All reactions (curves a, b and c) were performed at pH 6.0, with 20 mM phosphate buffer containing 100 μM H_2O_2, 100 mM NaCl, 95 μM NADPH and 18 nM MPO: reaction in the absence (curve a) or in the presence of 10 μM TNM (curve c); under argon flux (curve b). These absorbances decreased at a mean rate of 92 ± 5 μM/min, corresponding to a turnover rate of 85 ± 4 s^{-1} (curves a, b and c). After 4 min of reaction, 5 mM glucose 6-phosphate and 0.1 μM glucose-6-phosphate dehydrogenase were added to recycle the oxidized NADPH metabolite to NADPH, without success. Control experiments: 102 μM NADPH in buffer decreased at a rate of 0.3 μM/min (curve d); 101 μM NADPH in the presence of 1 μM MPO and 100 μM H_2O_2 (curve e) decreased at a rate of 8.2 μM/min, corresponding to a turnover rate of 0.14 s^{-1}.

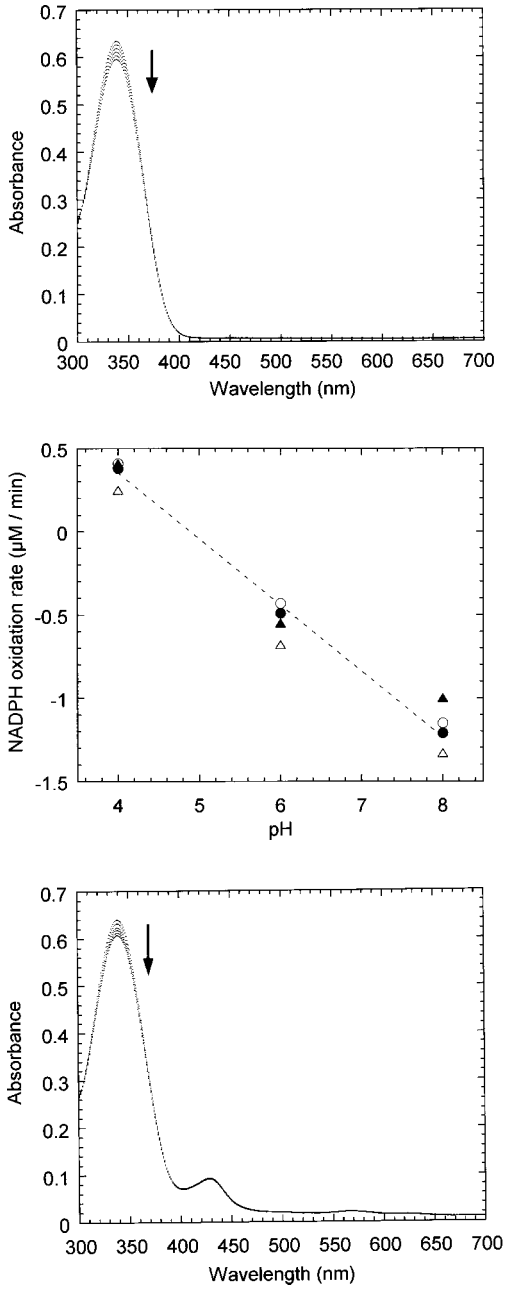

Figure 2 Spectral changes of NADPH solutions

Top and bottom panels: time-dependent spectra of an NADPH solution incubated for 20 min in 20 mM phosphate buffer, pH 6.0. Top panel: NADPH alone at 102 μM. Bottom panel: 103 μM NADPH in the presence of 1.1 μM MPO. The scans were taken at 4 min intervals. Arrows indicate the direction of spectral changes. Middle panel: effect of pH on the rate of NADPH consumption (μM/min, logarithmic scale) for NADPH in buffer with (○) or without (●) argon; for NADPH in the presence of 1 μM MPO with (△) or without (▲) argon.

spectral changes, as illustrated in Figure 2 (top panel). Over 20 min there was no measurable change in absorbance at 260 nm. In contrast, a decrease in A_{339} was observed at a rate of 0.32 ± 0.06 μM/min ($n = 10$), corresponding to 6% of the complete reaction (Figure 2, top panel). For purposes of comparison, this time course was added to the time scale of the chlorination reaction illustrated in Figure 1 (curve d). The addition of catalase, SOD or H_2O_2 had no effect on the rate. Similar variations were

Table 1 Comparison of the rate and extent of NADPH reactions under various conditions

All the reactions were performed at pH 6.0 in 20 mM phosphate buffer containing 100 μM NADPH. As necessary, the reaction was performed in the presence of 100 μM H_2O_2, or 100 μM H_2O_2 and 100 mM NaCl, or 100 μM free HOCl. MPO concentrations are indicated in the table. Results are means ± S.D. for *n* assays. n.d., not determined.

	NADPH alone in buffer	NADPH + 1 μM MPO	NADPH + 1 μM MPO + H_2O_2		NADPH + 0.018 μM MPO + H_2O_2 + NaCl		NADPH + HOCl	
	Rate (μM/min)	Rate (μM/min)	Rate (μM/min)	Extent (μM)	Rate (μM/min)	Extent (μM)	Rate (μM/min)	Extent (μM)
NADPH oxidation	0.32 ± 0.06 (n = 10)	0.28 ± 0.06 (n = 4)	8.7 ± 1.2 (n = 6)	26 ± 6 (n = 6)	94 ± 13 (n = 7)	100	Instantaneous	100
+ SOD (1 μM)	0.33	n.d.	4.3 ± 1.0 (n = 4)	28 ± 4 (n = 4)	0	0	0	0
+ TNM (10 μM)	n.d.	n.d.	n.d.	n.d.	99 ± 10 (n = 4)	100	Instantaneous	100
+ Argon	0.37	n.d.	4.2 ± 1.0 (n = 4)	22 ± 8 (n = 4)	100 ± 16 (n = 4)	100	Instantaneous	100
UV shift at 260 nm	No	No		No		Yes	Yes	
Coenzyme activity*	No	No		Yes		No	No	

* $NADP^+$ coenzyme activity was determined with 5 mM glucose 6-phosphate and 0.1 μM glucose-6-phosphate dehydrogenase.

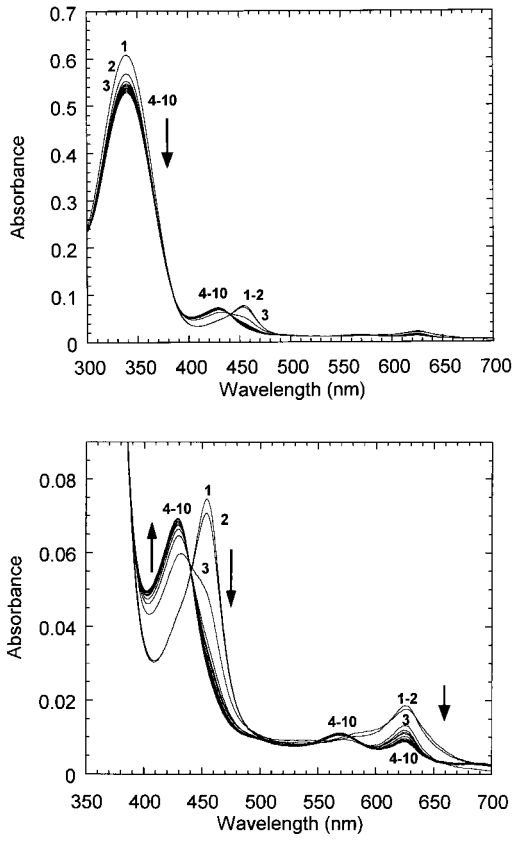

Figure 3 Spectral changes of NADPH solutions in the presence of MPO and H_2O_2

Time-dependent spectra of a 91 μM NADPH solution incubated in 20 mM phosphate buffer, pH 6.0, in the presence of 0.92 μM MPO and 100 μM H_2O_2. The scans were taken at 2 min intervals after the addition of H_2O_2, up to 20 min. Upper panel: spectra recorded over 400 nm. Lower panel: detail in the α and γ band of MPO, showing a constant A_{626}/A_{454} of 0.24. Arrows indicate the direction of spectral changes.

observed when solutions were thoroughly deoxygenated with argon (Table 1). The absence of any effect suggested that no oxidation process was involved in these absorbance changes. Variations of this rate as a function of pH under anaerobic conditions are shown in Figure 2 (middle panel). Although the reaction was 10-fold faster at pH 4.0, it remained negligibly small compared with the rates measured in the presence of Cl^-. It is of interest that after a 3.5 h incubation leading to a 51% decrease in the characteristic absorbance band of NADPH, the addition of the glucose-6-phosphate dehydrogenase system did not allow the regeneration of NADPH.

Spectral changes of NADPH in the presence of MPO

Next we examined in detail the aerobic reaction between MPO and NADPH. Without exogenously added H_2O_2, time-dependent spectra, illustrated in Figure 2 (bottom panel), showed that MPO remained in the native form for at least 20 min and no further reaction was observed between MPO and NADPH. We verified that whatever the pH in the range 8–4, there was no modification at 260 nm and a minimal absorbance decrease at 339 nm at a rate close to that detected previously, at the same pH, in the absence of MPO (Figure 2, middle panel). This observation is consistent with studies indicating that the oxi-

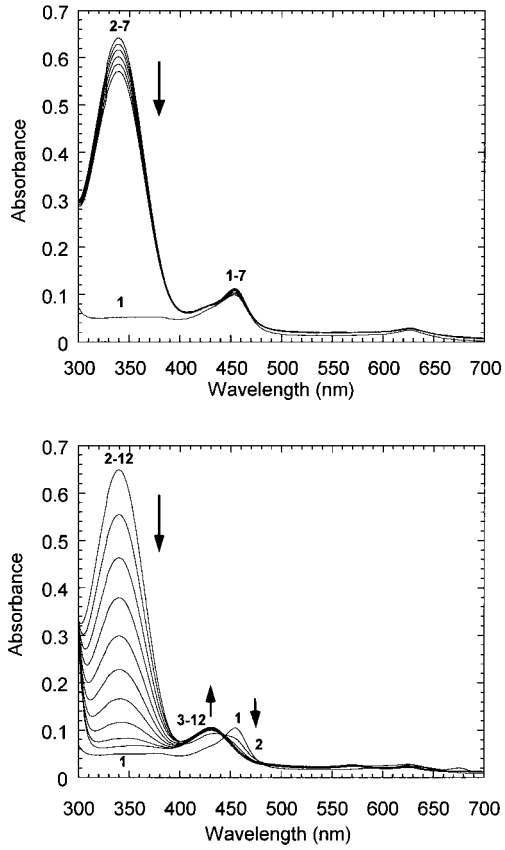

Figure 4 Reaction of C II with NADPH

C II was generated by the addition to 1.1 μM MPO of glucose oxidase to generate a constant flux of 5 μM H_2O_2/min in 20 mM phosphate buffer, pH 6.0, containing 45 mM glucose. Upper panel: spectral conversion on the addition of 100 μM NADPH. Lower panel: spectral conversion on the addition of 100 mM NaCl and 100 μM NADPH. Spectra were recorded before the addition of NADPH (curve 1), after the addition of NADPH (curve 2) and then at 3 min intervals. Arrows indicate the direction of spectral changes.

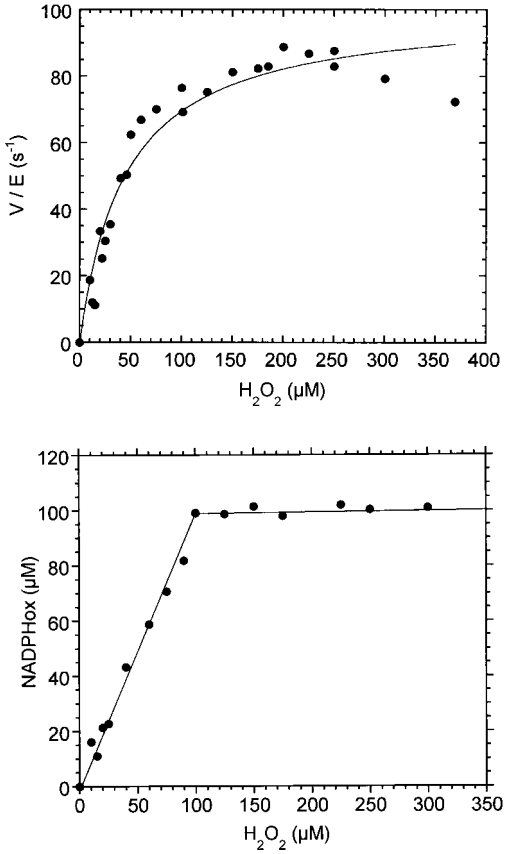

Figure 5 Effect of H_2O_2 concentration on the rate of NADPH oxidation

Upper panel: effect of H_2O_2 on the initial rate of NADPH oxidation, *V*/*E*, expressed as the molar concentration of NADPH disappearing/s per haem molar concentration of MPO. Reaction mixtures contained 20 nM MPO, 100 mM NaCl, 100 μM NADPH and various concentrations of H_2O_2 in 20 mM phosphate buffer, pH 6.0. The line through the points corresponds to a fit to the Michaelis–Menten relation giving $k_{cat} = 100 \pm 5$ s^{-1} and $K_m = 44 \pm 7$ μM. Lower panel: the effect of H_2O_2 on the maximum recorded yield of oxidized NADPH metabolite illustrated a total and equimolar reaction between H_2O_2 and NADPH.

dation of NADPH and the concomitant formation of peroxidase C III required small amounts of H_2O_2 [36–38].

Spectral changes of NADPH in the presence of MPO and H_2O_2

In contrast, when H_2O_2 was added to the solution (Figure 3, upper panel), the enzyme changed instantaneously into C II with the concomitant oxidation of NADPH. Analyses of A_{626}/A_{454}, which were 0.24 ± 0.02 ($n = 13$) and 0.24 ± 0.04 ($n = 7$) (mean $\pm$S.D.) in the absence and presence of NADPH respectively, did not permit the detection of a significant amount of C III (12%). After a short steady-state accumulation of C II, over 5 min, the MPO returned to the native form (Figure 3, lower panel). This accumulation of C II is consistent with the observation that horseradish peroxidase C II accumulates in the presence of NADH and H_2O_2 [39], which was contrary to the prevalent idea that horseradish peroxidase C III is the dominating species in the horseradish peroxidase/NADH system. The presence of MPO C II was synchronized with a rapid oxidation of NADPH at a mean rate of 8 μM/min followed by a slow decrease at 0.3 μM/min, close to the value of the control in buffer (Table 1). In the rapid phase the turnover rate was still lower (0.14 s^{-1}) than in the presence of Cl^- (88 s^{-1}), as illustrated by the time course in Figure 1 (scan e). The addition of catalase completely inhibited the rapid phase, whereas the addition of 1 μM SOD decreased the rate. Similarly, in the absence of O_2, the oxidation was substantially decreased (Table 1). The addition of glucose-6-phosphate dehydrogenase at the end of the rapid phase allowed the recovery of NADPH. Finally, in the presence of MPO and H_2O_2, the oxidation of NADPH proceeded at a low rate and with a low yield, corresponding to 0.26 ± 0.06 mol of NADPH oxidized by 1 mol of H_2O_2. Moreover, inhibition by SOD indicated that $O_2^{-\cdot}$ was a necessary intermediate in the reaction.

Peroxidase intermediate during steady-state reactions

The following steady-state experiments were performed to provide information on the enzyme form that predominated during NADPH oxidation. In the presence of glucose–glucose-oxidase as an H_2O_2-generating system, MPO was converted into C II within 1 min. Figure 4 demonstrates the spectral conversion on the addition of Cl^- or NADPH to preformed C II. On the addition of 100 μM NADPH, no shift in the position of C II was detectable (Figure 4, upper panel). With NADPH in the presence of 100 mM Cl^-, the dominating steady-state MPO intermediate changed instantaneously from C II (maxima at 454 and 626 nm) to native MPO (maximum at 428 nm) (Figure 4, lower panel).

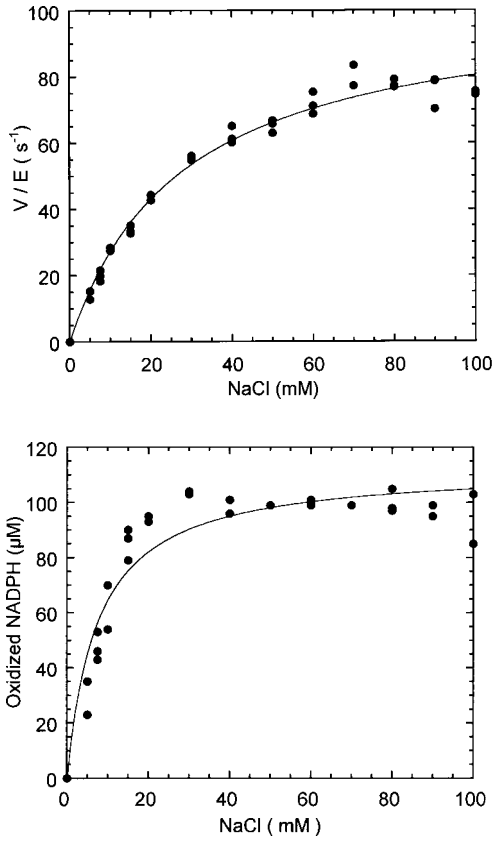

Figure 6 Effect of NaCl concentration on the rate and extent of NADPH oxidation

Upper panel: effect of NaCl on the initial rate of NADPH oxidation, *V*/*E*, measured in the presence of 110 μM NADPH, 100 μM H_2O_2, 28 nM MPO and various concentrations of NaCl from 1 to 300 mM in 20 mM phosphate buffer, pH 6.0. The line through the points corresponds to a fit to the Michaelis–Menten relationship, giving $k_{cat} = 103 \pm 3\ s^{-1}$ and $K_m = 28 \pm 2$ mM. Lower panel: dependence of the maximum recorded yield of oxidized NADPH on NaCl concentration, allowing an estimate of $K_d = 7.5 \pm 1.1$ mM, the concentration of NaCl yielding 50% of the maximal activity.

Table 2 Effect of pH on kinetic parameters for NaCl and on K_d

The k_{cat} and K_m values for NaCl were determined from fitting the data obtained for NADPH oxidation in the presence of MPO and 100 μM H_2O_2 as typically described for pH 6.0 in Figure 6 (upper panel). The K_d for Cl^- binding was estimated from fitting the data illustrated in Figure 6 (lower panel). The values are the means ± S.D.

pH	K_m (mM)	k_{cat} (s^{-1})	k_{cat}/K_m ($mM^{-1} \cdot s^{-1}$)	K_d (mM)
4	1.22 ± 0.54	27 ± 4	22	0.09 ± 0.03
5	4.4 ± 1.0	51 ± 4	11.6	1 ± 0.5
6	28 ± 2	103 ± 3	5	7.5 ± 1.1
7	210 ± 60	90 ± 6	0.47	96 ± 26
8	900 ± 140	42 ± 4	0.047	1000 ± 175

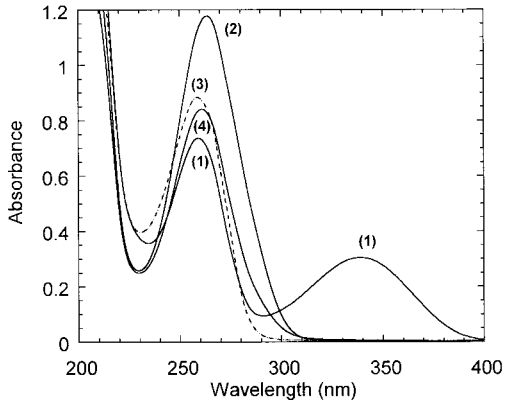

Figure 7 Absorption changes of NADPH on reaction with HOCl generated by the MPO/H_2O_2/Cl^- system

The reaction was performed at pH 6.0, with 20 mM phosphate buffer containing 100 mM NaCl, 17 nM MPO, 49 μM NADPH and added aliquots of 10 μM H_2O_2. Scan 1, NADPH without H_2O_2 (λ_{max} 259 nm); scan 2, NADPH metabolite after reaction with 1.22 H_2O_2 equivalents (λ_{max} 263 nm); scan 3, $NADP^+$ at 49 μM, the initial concentration of the reaction mixture (λ_{max} 259 nm); scan 4, NADPH metabolite after reaction with 2.8 H_2O_2 equivalents (λ_{max} 260 nm).

Thus Cl^- was very efficient in removing C II as the dominating steady-state species, whereas with NADPH the spontaneous reduction of C I to C II by H_2O_2 seemed to dominate over C I reduction to native MPO by NADPH.

Effects of various factors on the chlorination reaction

The effects of H_2O_2, Cl^- and pH on MPO activity have been studied by using NADPH oxidation as a probe. In earlier studies, the K_m for H_2O_2 was affected by the combined presence of Cl^- and pH conditions [23,25,40,41]. In the presence of 100 mM NaCl, when the H_2O_2 concentration was increased the initial rate of NADPH oxidation reached a maximum at 150–250 μM and then declined progressively. Under conditions of non-inhibiting H_2O_2 concentration, normal Michaelis–Menten kinetics with respect to the concentration of H_2O_2 was observed (Figure 5, upper panel). The apparent k_{cat} and K_m values for H_2O_2 were $100 \pm 5\ s^{-1}$ and $44 \pm 7\ \mu$M respectively at pH 6.0. When we analysed the variation in the extent of the reaction with H_2O_2 concentration, the maximal oxidation yield corresponded to a stoichiometry between H_2O_2 and oxidized NADPH of 1.07 ± 0.12 ($n = 29$), as typically illustrated in Figure 5 (lower panel).

Increasing the Cl^- concentration resulted in an increase in the rate of oxidized NADPH metabolite. At pH 6 the hyperbolic saturation curve fitted Michaelis–Menten kinetics with an apparent K_m of 28 ± 2 mM for Cl^- and a k_{cat} of $103 \pm 3\ s^{-1}$ (Figure 6, upper panel). A marked inhibition of the rate was noticed for Cl^- concentrations higher than 150 mM. The extent of NADPH oxidation increased with increasing concentration of NaCl and reached a plateau corresponding to the amount of added H_2O_2 at NaCl concentrations higher than 30 mM (Figure 6, lower panel). The half-saturation of the reaction rate allowed the definition of a dissociation constant, K_d, of 7.5 ± 1.1 mM at pH 6.0 for the MPO-Cl^- complex.

To optimize the experimental conditions, the dependence of the NADPH oxidation rate on Cl^- concentration was studied at various pH values and for 100 μM H_2O_2. Table 2 summarizes the kinetic parameters k_{cat} and K_m determined under conditions of non-inhibiting NaCl concentration and in the pH range 4–8, as well as K_d for the MPO–Cl^- complex. Optimal activity was obtained at pH 6. The corresponding catalytic efficiency (k_{cat}/K_m) of MPO for Cl^- decreased with increasing pH. Allowing for experimental errors, the K_m values were generally greater than the corresponding K_d values. The logarithms of the apparent K_m

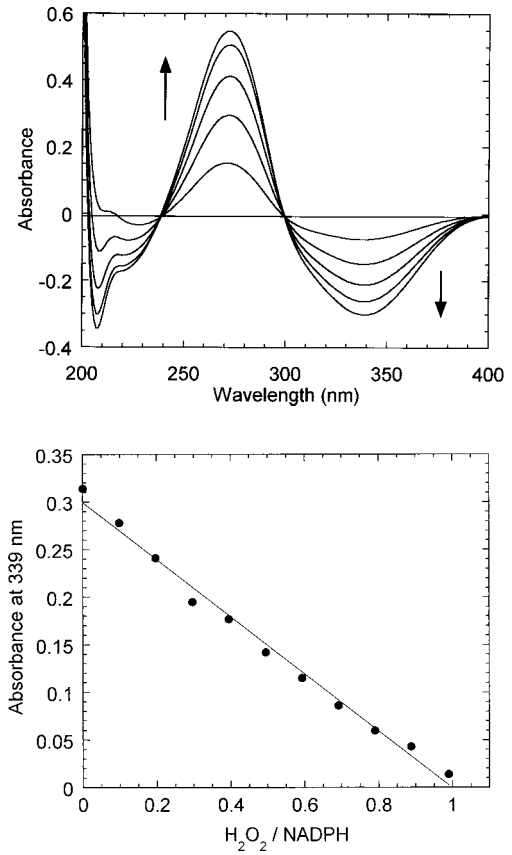

Figure 8 Difference spectra obtained after repetitive addition of H_2O_2 aliquots to NADPH in the presence of MPO and chloride

Upper panel: data were calculated from the difference between spectra recorded in the presence of H_2O_2, as in Figure 7, scan 2, and the initial spectrum of NADPH recorded without H_2O_2 (Figure 7, scan 1). Arrows indicate the growth and decay of each peak. From the *x*-axis in the direction of the arrows, scans correspond to 0.2, 0.41, 0.61, 0.81 and 1.22 H_2O_2 equivalents. The wavelength maxima are at 339 and 274 nm and the isosbestic points are at 300 and 238 nm. Lower panel: the addition of increasing amounts of H_2O_2 to NADPH causes a linear stoichiometric disappearance of the absorption band at 339 nm that extrapolates to 1.0 for the initial ratio of H_2O_2 to NADPH ($r^2 = 0.99$).

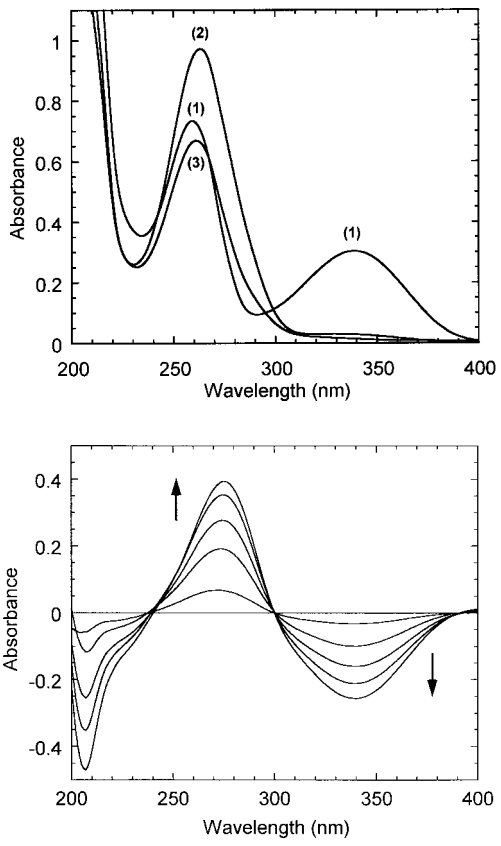

Figure 9 Absorption changes of NADPH on reaction with free HOCl

Upper panel: spectra obtained after the addition of 12 μM NaOCl aliquots to 51 μM NADPH in 20 mM phosphate buffer, pH 6.0. Scan 1, NADPH without NaOCl (λ_{max} 259 nm); scan 2, metabolite after reaction with 1.18 HOCl equivalents (λ_{max} 263 nm); scan 3, after reaction with 2.55 HOCl equivalents (λ_{max} 260 nm). Lower panel: difference spectra calculated after the serial addition of NaOCl aliquots. Arrows indicate the growth and decay of each peak. From the *x*-axis in the direction of the arrows, scans correspond to 0.12, 0.33, 0.54, 0.72 and 0.98 HOCl equivalent. The wavelength maxima are at 339 and 274 nm and the isosbestic points are at 300 and 238 nm.

and K_d increased linearly with pH with slopes of 0.74 ($r^2 = 0.99$) and 1.00 ($r^2 = 0.99$) respectively (results not shown).

We checked that the rate of NADPH oxidation was independent of NADPH concentration, when greater than 40 μM, and was thus totally dependent on the turnover of MPO (results not shown).

Spectral characterization of the oxidized NADPH metabolites

Reaction of NADPH with the MPO/H_2O_2/Cl^- system

Spectral changes recorded during the Cl^--dependent oxidation of NADPH by MPO/H_2O_2 are shown in Figure 7. By the addition of one molar equivalent of H_2O_2, NADPH (scan 1) was converted into a product (scan 2) other than $NADP^+$ (scan 3). Difference spectra (Figure 8, upper panel) obtained after the repetitive addition of H_2O_2 aliquots showed that the decrease in A_{339} was synchronized with the concurrent formation of a peak with an absorbance maximum at 274 nm, defined by a variation in absorbance coefficient, $\Delta\epsilon_{274}$, of 11.8 ± 1.3 $mM^{-1} \cdot cm^{-1}$ ($n = 18$). The presence of isosbestic points at 300 and 238 nm that were maintained throughout this titration, different from those of the NADPH/$NADP^+$ couple at 279 and 222 nm respectively, was probably consistent with the formation of a stable new metabolite, as confirmed by HPLC chromatography (A. Auchère, I. Artaud and C. Capeillè-Blandin, unpublished work). Titration results indicated that the complete disappearance of the 339 nm absorption band was obtained for an initial H_2O_2-to-NADPH ratio of 1.09 ± 0.12 ($n = 10$), as typically illustrated in Figure 8 (lower panel).

Further addition of H_2O_2 equivalents induced an decrease in A_{263} with a shift in the maximum to 260 nm and a loss of the previous isosbestic points, which was indicative of further reaction of the primary product by the action of HOCl generated by the enzyme (Figure 7, scan 4). Neither the primary product nor the final product exhibited the absorbance spectrum of $NADP^+$; in addition, neither product could be converted back into NADPH by the addition of glucose-6-phosphate dehydrogenase and glucose 6-phosphate.

Reaction of NADPH with HOCl

HOCl was most effective in supporting rapid NADPH oxidation, as shown from spectral changes recorded in the course of a redox

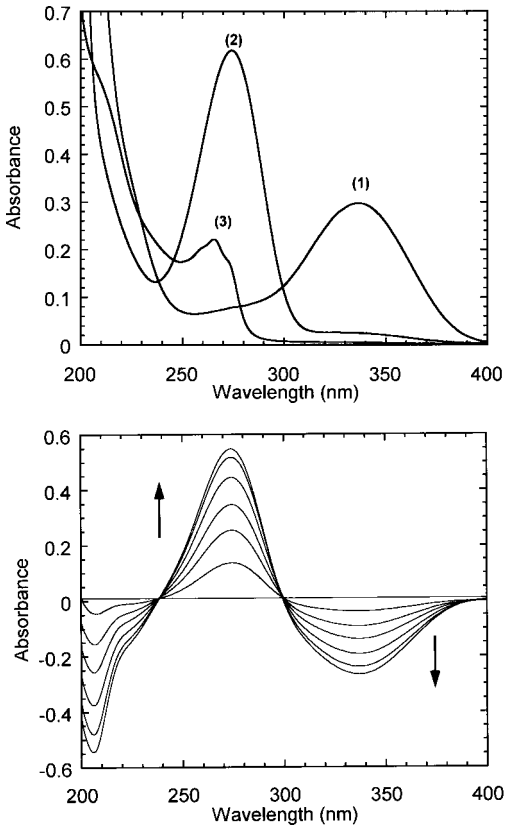

Figure 10 Absorption changes of NMNH on reaction with HOCl generated by the MPO/H_2O_2/Cl^- system

Upper panel: the reaction was performed at pH 6.0, with 20 mM phosphate buffer containing 100 mM NaCl, 18 nM MPO, 49 μM NMNH and added aliquots of 10 μM H_2O_2. Scan 1, NMNH without H_2O_2; scan 2, NMNH metabolite after reaction with 1.22 H_2O_2 equivalents; scan 3, NMN at 49 μM. Lower panel: difference spectra calculated after the serial addition of H_2O_2 aliquots. Arrows indicate the growth and decay of each peak. From the *x*-axis in the direction of the arrows, scans correspond to 0.2, 0.4, 0.59, 0.78, 0.96 and 1.14 H_2O_2 equivalents. The wavelength maxima are at 339 and 274 nm and the isosbestic points are at 300 and 238 nm.

titration of NADPH by HOCl (Figure 9, upper panel, scan 2). As shown by difference spectroscopy (Figure 9, lower panel), the decrease in A_{339} and the increase in A_{274} were in parallel, the maximum of the latter being reached with the full bleaching of the reduced nicotinamide obtained at a stoichiometry of 1.10 ± 0.19 ($n = 16$) between HOCl and NADPH (results not shown). All the spectra clearly showed the presence of isosbestic points at 300 and 238 nm. The variation in A_{274} corresponded to a $\Delta\epsilon$ of 11.2 ± 1.9 $mM^{-1} \cdot cm^{-1}$ ($n = 8$). This product still did not act as a cofactor for the assay system glucose-6-phosphate dehydrogenase and glucose 6-phosphate. We observed that the oxidation by HOCl was inhibited by SOD (Table 1). Thermodynamic considerations predict that HOCl is a poor one-electron oxidizing agent and reactions yielding radical species are not feasible [42]. Moreover, modifications of SOD by HOCl have been reported previously [43], so SOD was not considered to be a convenient tool in the present work. It is hoped that further investigations, currently in progress, will provide the answer to this question.

Reactions of NADPH analogues with HOCl

To clarify the part of the NADPH molecule on which the modification took place, we first performed experiments with various oxidized nucleotides, including $NADP^+$, NMN, deamino-$NADP^+$ and the adenine derivatives AMP and adenosine 2′,5′-diphosphate. After a 15 min incubation, either with one NaOCl equivalent or in the presence of the complete system, MPO/H_2O_2/Cl^- at one equivalent of H_2O_2, no spectral change in the characteristic absorption bands of pyrimidine bases at 260 nm was recorded. With $NADP^+$, after incubation at one HOCl equivalent, reaction with the glucose-6-phosphate dehydrogenase system was allowed, thus indicating that the coenzyme, still recognized, had not been oxidatively degraded further (results not shown).

When we performed similar studies with NMNH, a shift and an increase in the UV spectrum were noticed. Interestingly, by difference spectroscopy, when H_2O_2 was added step by step, the spectral variations were similar to those obtained with NADPH [Figures 8 (upper panel) and 10]. Indeed, isosbestic points at 300 and 238 nm were clearly visible, together with the formation of an oxidized NMNH metabolite characterized by a λ_{max} at 274 nm with a maximal spectral change obtained when the A_{339} had disappeared for one equivalent.

Table 3 summarizes the stoichiometry of the reactions of NADPH and NMNH with free HOCl or HOCl generated by the MPO/H_2O_2/Cl^- system as monitored at 339 nm, together with the spectral characterizations of the oxidized metabolite generated with a λ_{max} at 274 nm. These results suggest that the enzymic chlorinating system produced a well-defined intermediate with one molar equivalent of H_2O_2, analogous to the HOCl-supported reaction. Moreover, whereas experiments with different adenine analogues showed no coenzyme modifications, spectroscopically identical species were produced by the reaction of NMNH and NADPH with the MPO/H_2O_2/Cl^- system, thus indicating that chlorination occurred on the nicotinamide part of the NADPH molecule.

Table 3 Reaction of HOCl, both free and generated by the MPO/H_2O_2/Cl^- system, with NADPH and NMNH: stoichiometry and spectral characterizations of the metabolite

Data were deduced from typical difference spectra illustrated in Figures 8, 9 and 10. Stoichiometric values, *n* being the ratio of the oxidant to the reduced nucleotide, were calculated from linear relationships leading to the complete loss of A_{339}, as illustrated typically in Figure 8 (lower panel). Values of $\Delta\epsilon$ at the λ_{max} of 274 nm were calculated from the maximal absorbance changes synchronized with the disappearance of A_{339}. Results are means $\pm$ S.D. for the numbers of assays shown in parentheses.

Cofactor	H_2O_2/reduced nucleotide	HOCl/reduced nucleotide	$\Delta\epsilon_{274}^{max}$ ($mM^{-1} \cdot cm^{-1}$) for enzymic reaction	$\Delta\epsilon_{274}^{max}$ ($mM^{-1} \cdot cm^{-1}$) for HOCl titration
NADPH	1.09 ± 0.12 (10)	1.10 ± 0.19 (16)	11.8 ± 1.3 (18)	11.2 ± 1.9 (8)
NMNH	1.11 ± 0.15 (5)	1.00 ± 0.13 (3)	11.0 ± 1.2 (6)	11.2 ± 2.8 (6)

DISCUSSION

The present study used NADPH to examine the effect of pH, H_2O_2 and Cl^- concentration on the chlorinating activity of human MPO. It is well established that, although the oxidation of NAD(P)H by horseradish peroxidase/H_2O_2 or by MPO/H_2O_2 is very slow, it requires the presence of a mediating molecule, acting as a redox catalyst for NAD(P)H oxidation, for it to be greatly enhanced [31,36,44–47]. Indeed, our results indicate that the chloride oxidation product, HOCl, stimulated NADPH oxidation, which is totally dependent on the turnover of MPO, and promotes the irreversible formation of an oxidized NADPH metabolite.

To provide a basis for interpreting the oxidation of NADPH by HOCl, evidence for the occurrence of a reaction different from the oxidation to $NADP^+$ was obtained by analyses of the effects of various factors and the coenzyme activities of the reaction products (Table 1). Several lines of evidence allowed us to distinguish between various possible mechanisms of NADPH consumption. Previous reports on the instability of NADH and NADPH solutions showed that the slow acid-catalysed spectral changes at 339 nm represented α–β epimerization at the nicotinamide–riboside bond [48]. Our results indicated that in fact the spectral changes observed in buffered NADPH solutions, which could occur under anaerobic conditions and in the presence of catalase, SOD or H_2O_2, were not related to the oxidation of NADPH to $NADP^+$ but involved a process that was strongly dependent on the acid concentration. Consistent with the above interpretation was the observation that the metabolite generated had no coenzyme activity with glucose-6-phosphate dehydrogenase.

It is of interest that, in the presence of MPO, spectral changes similar in their rate and extent were maintained and the enzyme remained in the native form. No reaction between peroxidase and NADPH could be detected. In contrast, a slight O_2 consumption of 1.5 μM/min, corresponding to a turnover rate of 0.22 s^{-1}, had been previously reported [49]. In a later paper, the same authors demonstrated the presence of H_2O_2 in their phosphate buffers [50]. Taken together, the results became consistent with previous studies indicating that the peroxidase-catalysed oxidation of NAD(P)H by O_2 required small amounts of H_2O_2 [36–38], which could be present in aerobically prepared solutions owing to a slow autoxidation process [51]. In the present study this disagreement was avoided by the use of freshly prepared NADPH solutions.

Indeed, MPO needed an exogenous source of H_2O_2 for significant catalysis of the oxidation of NADPH. The normal active $NADP^+$ was generated, whereas the reaction product obtained in the presence of Cl^- did not show any coenzyme activity with the glucose-6-phosphate dehydrogenase system. A comparison of the effects of O_2 and SOD in the presence of the MPO/H_2O_2 system emphasized the contribution of both a peroxidase and an oxidase reaction in the oxidation of NADPH. In the former, a two-electron reaction would be preferentially involved between C I and NADPH to produce $NADP^+$ and the native enzyme. Conversely, as in the classic peroxidase cycle [eqns. (3) and (4)], the stepwise reduction of C I by NADPH would produce C II and an $NADP^{\bullet}$ radical. Thus the resulting radical could initiate a non-enzymic oxidative cycle in which O_2 could be reduced to $O_2^{-\bullet}$ [52] and dismutate to H_2O_2. Once such a chain propagation was initiated, $NADP^{\bullet}$ production would be the rate-limiting step and NADPH oxidation would proceed to completion. Indeed, similar results were reported when NAD(P)H oxidation was mediated by phenoxyl radicals generated by specific substrates of the peroxidase such as tyrosine, scopoletin, thyroxine and paracetamol [31,39,44,45]. In the present study, the occurrence of a reaction with a low yield and at a low rate suggests that the reactivity of NADPH with MPO intermediates is probably very low compared with that of the phenolic substrates. This interpretation is strengthened by the accumulation of C II as a steady-state intermediate in the presence of a H_2O_2-generating system. Therefore the value of the rate constant for C I reduction by NADPH should be at least one or two orders of magnitude lower than the rate constant for C I reduction by H_2O_2. Moreover, NADPH is unable to compete effectively with Cl^-. Indeed, in the presence of Cl^- MPO exists mainly in the native state. This is consistent with the known reactivity of C I, which is greater with Cl^- [eqn. (2)] (4.7×10^6 $M^{-1} \cdot s^{-1}$) [47] than with H_2O_2 [eqn. (3)] (8.2×10^4 $M^{-1} \cdot s^{-1}$) [53,54].

In contrast, in the presence of Cl^- no evidence could be found for the formation of reactive free-radical intermediates in the oxidation of NADPH. If $NADP^{\bullet}$ radicals had been generated, they would have reacted with oxygen to form $NADP^+$ and $O_2^{-\bullet}$ [52]. If there is any formation of the radical, its extent seems to be very small because it cannot be detected by reduction of NBT or TNM. The reaction does not need O_2 and can occur under argon, so it is not an oxidase-catalysed reaction. Consistent with this interpretation is the finding that the stoichiometric ratio of the disappearance of NADPH to that of H_2O_2 was to be less than or equal to 1. If there were a contribution to an aerobic NADPH oxidation by the MPO/H_2O_2 system, the stoichiometry of oxidized NADPH to added H_2O_2 would expected to be greater than 1, as observed for tyrosine-mediated NADPH oxidation by the MPO/H_2O_2 system [31]. Consequently, our results suggest that the stimulated oxidation of NADPH by HOCl involves a reaction with a two-electron-oxidized metabolite of Cl^- and not a radical chain propagation.

All the evidence indicates that free HOCl is the enzymically produced oxidized halogen species. The proposal of the occurrence of a similar reaction in the presence of the MPO/H_2O_2/Cl^- system and in the presence of free HOCl was based on similarities between the reaction products, as characterized by the same spectral changes obtained in the course of their reaction. Indeed, the absorbance spectra of the reaction products seemed identical in their λ_{max} positions, $\Delta\epsilon$ values and isosbestic points, regardless of the means of oxidation. These findings confirm and extend earlier observations that free hypohalite acts as the halogenating agent in the chlorination reactions of MPO [13,18,22,40]. It can be concluded that chlorination takes place on NADPH, resulting in catalytically inactivated products. On the basis of the known reactivity of HOCl, promoting the formation of chloramines and chlorohydrins [6,8–10], there are two possible sites on NADPH for halogenation: the amino group of the adenine moiety and the unsaturated carbon double bond of the reduced nicotinamide moiety. Interestingly, the changes in the absorbance spectra of NADPH are quantitatively similar to those that occur in NMNH once the contribution of the adenine chromophore of the compound has been removed from the absorbance curve. The most logical interpretation of this striking similarity in absorbance spectra of the chlorinated metabolites is the occurrence of a similar mechanism, not involving the adenine moiety but at the level of the nicotinamide moiety. Efforts to identify conclusively the products of the enzymic reaction of NADPH with H_2O_2 and Cl^- and to establish their chemical structures are in progress by reverse-phase HPLC, MS and NMR.

Several lines of evidence indicate that NADPH is most effective in accounting for the major characteristics of the complex chlorination reaction and has useful properties for evaluation of

the chlorinating activity of MPO. In the reaction catalysed by MPO, NADPH is oxidized almost quantitatively after a monophasic exponential decay, i.e. the amount of oxidized NADPH metabolite produced after H_2O_2 had been consumed revealed that 93 % of the amount of H_2O_2 added to the reaction mixture was converted into HOCl. This property is essential to a conclusion that the measurement of HOCl by oxidation of NADPH is an accurate representation of HOCl production by MPO. It should be recalled that this did not occur when MCD was used to scavenge HOCl. Moreover, the steady-state rate depended on the observation time scale, as discussed in [24,25]. The real enzymic activity was at most 20 % of that with NADPH under similar conditions and was therefore grossly underestimated.

The complex kinetic pattern of the chlorination reaction catalysed by MPO has been documented in several reports. Cl^- not only acts as a substrate for MPO but also behaves as a competitive inhibitor of H_2O_2 [12]. With the use of NADPH as a coupled reaction, the effect of Cl^- or H_2O_2 on the oxidation of NADPH exhibited saturation kinetics close to that established with other coupled reactions; inhibitory effects on the rate were observed at high concentrations. From the present results, a K_m for H_2O_2 of 44 μM was estimated at pH 6.0 and 100 mM Cl^-. This value is in reasonnable agreement with the determination reported previously, with TMB as a HOCl scavenger, yielding a value of 32 μM [41], but is slightly less than the 70 μM reported with MCD [23] and the 100 μM estimated by extrapolation of the data presented in [40] to 100 mM NaCl, with diethanolamine to detect chlorination at pH 6.0.

As expected, k_{cat}/K_m for H_2O_2 determined in the presence of NaCl (2.3×10^6 $M^{-1} \cdot s^{-1}$) was an order of magnitude lower than the rate constant determined for C I formation in the absence of NaCl by transient methods [54,55]. Indeed, the decrease in k_{cat}/K_m reflects the competition of Cl^- with H_2O_2 for the native enzyme [23,40,41].

Chlorination is known to be regulated by an acid/base group with a pK_a of 4.3. When protonated, it prevents the reaction of the enzyme with peroxides and favours the binding of halides [19,23,25,41,55]. Thus the position of the optimal pH in enzymic activity is governed by the NaCl-to-H_2O_2 ratio. We have confirmed that when using a ratio of 10^3 the chlorinating activity of MPO is greater at pH 6.0. This pH value is in good agreement with the pH optimum of 6.5 and 5.8 reported respectively in [56] and [40] for the same ratio, using H_2O_2 loss and diethanolamine respectively to detect chlorination.

The present results confirmed that the logarithm of the K_m for Cl^- increased linearly with pH, with a slope of 0.74. A similar dependence was also observed in the chlorination of MCD by MPO (0.84), as reported in [23]. At pH 6.0 and for 100 μM H_2O_2, our experimental value of 28 mM for the K_m of chloride is equal to that estimated by extrapolation of the data determined by diethanolchloramine formation [40]. However, a large discrepancy is noticed with the 200 mM estimated from the MCD assay at 166 μM H_2O_2 reported by [23].

It is of interest that the kinetic parameters determined at pH 7.0 with NADPH (Table 2) are in good agreement with those obtained after H_2O_2 loss in accounting for the chlorination activity of MPO, namely $K_m = 175$ mM and $k_{cat} = 79$ s^{-1} at pH 7.4 [57]. This assay was highly recommended [56] but required an oxidase meter fitted with an oxidase probe.

The dissociation constant of the MPO–Cl^- complex, as determined from the spectral changes induced by the addition of Cl^- to MPO, varies widely with pH, from 0.3 mM at pH 4.0 to 1.35 M at pH 8.0 [55]. These values are in agreement with our determinations obtained directly from analyses of the extent of NADPH oxidation with Cl^- concentration (Table 2). Moreover, a similar linear relationship was established between pH and the pK_d for Cl^-, in the pH range 4–8.

Finally, on the basis of the results presented here, we conclude that the NADPH assay described here can supplement other methods such as the monitoring of H_2O_2 consumption during HOCl generation by MPO. It has several advantages over spectrophotometric methods previously reported with the use of MCD or L-ascorbic acid. Unlike these molecules, which detect HOCl, NADPH has no significant reactivity towards the enzyme intermediates of MPO and therefore the decrease in the steady-state concentration of NADPH by such side-reactions is negligibly small and does not influence the enzyme chlorination activity. Chlorination of NADPH allows a continuous monitoring of the generation of HOCl and is relatively sensitive and specific, permitting the determination of kinetic and thermodynamic parameters. Our studies have revealed that the formation of chlorinated metabolites is irreversible, whereas in the cell $NADP^+$ is recycled enzymically. It is therefore possible that these new metabolites are unique for oxidation by HOCl and thus provide potential useful markers of HOCl production. Their detection *in vivo* would strongly support the involvement of MPO in inflammatory tissue damage.

REFERENCES

1 Klebanoff, S. J. (1988) in Inflammation: Basic Principles and Clinical Correlates (Gallin, J. I., Golstein, I. M. and Snyderman, R., eds.), pp. 391–444, Raven Press, New York
2 Winterbourn, C. C. (1990) in Oxygen Radicals: Systemic Events and Disease Processes (Das, D. K. and Essman, W. B., eds.), pp. 31–70, Karger, Basel
3 Thomas, E. L. and Learn, D. B. (1991) in Peroxidases in Chemistry and Biology, vol. 1 (Everse, J., Everse, K. E. and Grisham, M. B., eds.), pp. 83–104, CRC Press, Boca Raton, FL
4 Naskalski, J. W., Stelmaszynska-Zgliczynska, T., Drozdz, R. and Olszowska, E. (1995) Klin. Biochem. Metab. **3**, 3–8
5 Kettle, A. J. (1996) FEBS Lett. **379**, 103–106
6 Bernofsky, C. (1991) FASEB J. **5**, 295–300
7 van Zyl, J. M., Basson, K., Kriegler, A. and van der Walt, B. J. (1991) Biochem. Pharmacol. **42**, 599–608
8 Prutz, W. A. (1996) Arch. Biochem. Biophys. **332**, 110–120
9 Winterbourn, C. C., van den Berg, J. J. M., Roitman, E. and Kuypers, F. A. (1992) Arch. Biochem. Biophys. **296**, 547–555
10 Heinecke, J. W., Li, W., Mueller, D. M., Bohrer, A. and Turk, J. (1994) Biochemistry **33**, 10127–10136
11 Klebanoff, S. J. (1991) in Peroxidases in Chemistry and Biology, vol. 1 (Everse, J., Everse, K. E. and Grisham, M. B., eds.), pp. 1–35, CRC Press, Boca Raton, FL
12 Hurst, J. K. (1991) in Peroxidases in Chemistry and Biology (Everse, J., Everse, K. E. and Grisham, M. B., eds.), pp. 37–62, CRC Press, Boca Raton, FL
13 Winterbourn, C. C. (1985) Biochim. Biophys. Acta **840**, 204–210
14 Chesney, J. A., Mahoney, J. R. and Eaton, J. W. (1991) Anal. Biochem. **196**, 262–266
15 Ching, T. L., de Jong, J. and Bast, A. (1994) Anal. Biochem. **218**, 377–381
16 Tsan, M. F. (1982) Infect. Immun. **36**, 136–141
17 Turkall, R. M. and Tsan, M. (1982) J. Reticuloendothel. Soc. **31**, 353–360
18 Capeillère-Blandin, C., Martin, C., Gaggero, N., Pasta, P., Carrea, G. and Colonna, S. (1998) Biochem. J. **335**, 27–33
19 Stelmaszynska, T. and Zgliczynski, J. M. (1974) Eur. J. Biochem. **45**, 305–312
20 Weiss, S. J., Klein, R., Slivka, A. and Wei, M. (1982) J. Clin. Invest. **70**, 598–607
21 Marquez, L. A. and Dunford, H. B. (1994) J. Biol. Chem. **269**, 7950–7956
22 Harrisson, J. E. and Schultz, J. (1976) J. Biol. Chem. **251**, 1371–1374
23 Bakkenist, A., De Boer, L. E. G., Plat, H. and Wever, R. (1980) Biochim. Biophys. Acta **613**, 337–348
24 Kettle, A. J. and Winterbourn, C. C. (1988) Biochim. Biophys. Acta **957**, 185–191
25 Zuurbier, K. W. M., Bakkenist, A. R. J., Wever, R. and Muijers, A. O. (1990) Biochim. Biophys. Acta **1037**, 140–146
26 Bolscher, B. G., Zoutberg, G. R., Cuperus, R. A. and Wever, R. (1984) Biochim. Biophys. Acta **784**, 189–191
27 Marquez, L. A., Dunford, H. B. and Van Wart, H. (1990) J. Biol. Chem. **265**, 5666–5670

28 Selvaraj, R. J., Zgliczynski, J. M., Paul, B. B. and Sbarra, A. J. (1980) J. Reticuloendothel. Soc. **27**, 31–38
29 Griffin, B. W. and Haddox, R. (1985) Arch. Biochem. Biophys. **239**, 305–309
30 Virion, A., Michot, J. L., Deme, D. and Pommier, J. (1985) Eur. J. Biochem. **148**, 239–243
31 Capeillère-Blandin, C. (1998) Biochem. J. **336**, 395–404
32 Bakkenist, A. R. J., Wever, R., Vulsma, T., Plat, H. and Van Gelder, B. F. (1978) Biochim. Biophys. Acta **524**, 45–54
33 Hoogland, H., Van Kuilenburg, A., Van Riel, C., Muijsers, A. O. and Wever, R. (1987) Biochim. Biophys. Acta **916**, 76–82
34 Beers, Jr., R. F. and Sizer, I. W. (1952) J. Biol. Chem. **195**, 133–140
35 Morris, J. C. (1966) J. Phys. Chem. **70**, 3798–3805
36 Klebanoff, S. J. (1960) Biochim. Biophys. Acta **44**, 501–509
37 Yokota, K. and Yamazaki, I. (1965) Biochim. Biophys. Acta **105**, 301–312
38 Saikumar, P., Swaroop, A., Ramakrishna Kurup, C. K. and Ramasarma, T. (1994) Biochim. Biophys. Acta **1204**, 117–123
39 Marquez, L. A. and Dunford, H. B. (1995) Eur. J. Biochem. **233**, 364–371
40 Zgliczynski, J. M., Selvaraj, R. J., Paul, B. B., Stelmaszynska, T., Poskitt, P. K. F. and Sbarra, A. J. (1977) Proc. Soc. Exp. Biol. Med. **154**, 418–422
41 Andrews, P. C. and Krinski, N. I. (1982) J. Biol. Chem. **257**, 13240–13245
42 Koppenol, W. H. (1994) FEBS Lett. **347**, 5–8
43 Sharonov, B. P. and Dhurilova, I. V. (1992) Biochem. Biophys. Res. Commun. **189**, 1129–1135
44 Takayama, T. and Nakano, M. (1977) Biochemistry **16**, 1921–1926
45 Keller, R. J. and Hinson, J. A. (1991) Drug Metab. Dispos. **19**, 184–187
46 Michot, J. L., Virion, A., Deme, D., De Prailaune, S. and Pommier, J. (1985) Eur. J. Biochem. **148**, 441–445
47 Marquez, L. A. and Dunford, H. B. (1995) J. Biol. Chem. **270**, 30434–30440
48 Miles, D. W., Urry, D. W. and Eyring, H. (1968) Biochemistry **13**, 2333–2338
49 Svensson, B. E. and Lindvall, S. (1988) Biochem. J. **249**, 521–530
50 Svensson, B. E. (1988) Biochem. J. **256**, 751–755
51 Bernofsky, C. and Wanda, S. C. (1982) J. Biol. Chem. **257**, 6809–6817
52 Land, E. J. and Swallow, A. J. (1971) Biochim. Biophys. Acta **234**, 34–42
53 Hoogland, H., Dekker, H. L., van Riel, C., van Kuilenburg, A., Muijers, A. O. and Wever, R. (1988) Biochim. Biophys. Acta **955**, 337–345
54 Marquez, L. A., Huang, J. T. and Dunford, H. B. (1994) Biochemistry **33**, 1447–1454
55 Bolscher, B. G. and Wever, R. (1984) Biochim. Biophys. Acta **788**, 1–10
56 Kettle, A. J. and Winterbourn, C. C. (1989) Biochem. J. **263**, 823–828
57 van Dalen, C. J., Whitehouse, M. W., Winterbourn, C. C. and Kettle, A. J. (1997) Biochem. J. **327**, 487–492

Received 8 February 1999/12 July 1999; accepted 13 August 1999